Influence of polar surface properties on InGaN/GaN core-shell nanorod LED properties

M. Auf der Maur, F. Sacconi and A. Di Carlo
Dept. of Electronic Engineering
University of Rome "Tor Vergata", Italy
Email: auf.der.maur@ing.uniroma2.it

***Abstract*—InGaN/GaN nanorod core-shell LEDs have shown to be very promising candidates for high efficiency lighting devices. Such nanorods can be grown in different ways, leading to different device geometry and in particular to different structures near the polar Ga- and N-face nanorod surfaces. In this work the influence of the properties of the polar surfaces on the electrical device behaviour is studied qualitatively based on a semiclassical simulation model.**

I. Introduction

InGaN/GaN core-shell nanorod LEDs have many advantages over planar devices [1]. First, the effective light emitting area of nanorods can be considerably higher than in planar LEDs. Second, their 3-dimensional nature leads to an efficient elastic strain relaxation and to nearly defect-free structures. Third, most of the quantum well (QW) area is provided by the lateral non-polar wells. Therefore, the problems connected to the built-in polarization fields in nitride LEDs grown along the c-axis are mostly eliminated without the need of expensive non-polar GaN substrates.

Core-shell nanorods can be grown in different ways, leading to different device structures. Numerical simulations are a valuable tool for the detailed understanding of the electrical and optical behaviour of these structures and for the identification of the most efficient ones. Several simulation studies on core-shell LEDs have been presented recently [2], [3], [4], [5], focusing on a detailed description of electroluminescence, the contributions from polar and non-polar wells or on device optimisation. In this work we propose a study on the qualitative influence of the properties of the polar nanorod surfaces and nanorod termination.

Device behaviour can be influenced by three different properties connected to the polar nanorod surfaces. First, in particular in the case of free polar surfaces, strong local strain relaxation leads to a band gap lowering and thus potentially to increased carrier densities near the surfaces. Second, the discontinuity in the polarization field at the surface tends to induce electron and hole accumulation layers at the N- and Ga-face surfaces, respectively. And third, there can be recombination centers at the surfaces leading to non-radiative losses. These effects could be important in nanorod devices especially in the case of limited aspect ratio.

The simulations are based on continuous linear elasticity theory and the drift-diffusion model.

II. Simulation results

Simulations have been performed on the four structures shown in Fig. 1. An $In_{0.2}Ga_{0.8}N$/GaN MQW stack with 3

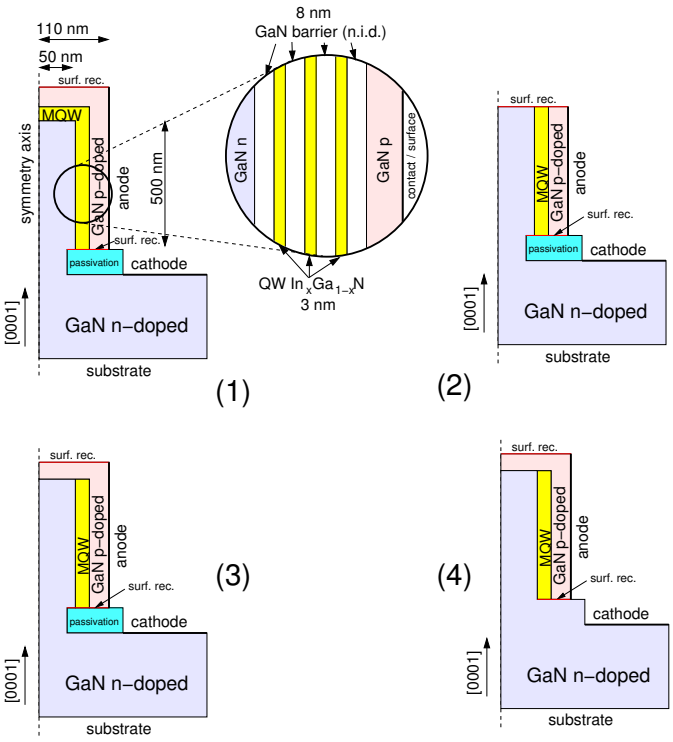

Fig. 1: The simulated InGaN/GaN MQW nanorod LEDs. Circular symmetry has been assumed.

QWs is grown on a 100 nm diameter n-doped GaN core, followed by a p-doped contact layer. In the first structure the InGaN QWs are grown all around the GaN core, such that the device includes polar c-plane QWs at the top end. The second structure assumes that these polar QWs are removed or avoided, such that the QWs extend to the top polar surface. The third structure is based on the second one, assuming however that the p-doped GaN shell is grown also on the top of the nanorod. These first three structures additionally assume a passivation layer on top of the GaN substrate so that the shell is isolated from the n-doped substrate. The fourth structure is based on the third, without the passivation layer. Additionally, we performed a set of simulations on the same

978-1-4673-1604-0/12/$31.00 ©2012 IEEE

devices including a surface recombination of Shockley-Read-Hall (SRH) type at the polar nanorod surfaces with surface recombination velocity of 10^4 cm/s, as indicated in Fig. 1. For all simulations we assumed the anode on the nanorod sidewall.

In the drift-diffusion simulation we consider radiative, SRH and Auger recombinations, with $B = 5 \times 10^{-11}$ cm^3/s, $\tau_{\mathrm{SRH}} = 20$ ns (inside the active intrinsic region, $\tau_{\mathrm{SRH}} \ll 1$ ns in the highly doped regions) and $C = 3 \times 10^{-31}$ cm^6/s, respectively. We assume a cylindrically symmetric device and simulate therefore a 2D slice.

Fig. 2 shows the simulated IV characteristics of the different devices. The first three devices present only slightly differing characateristics. The fourth one shows lower current first and a higher one after turn on. The former is due to the fact that the nanorod grown directly on GaN does not present an electron accumulation layer at the bottom nanorod interface due to the absence of a polarization field discontinuity on most of the interface. The higher turn on current is explained by the parasitic pn-junction at the bottom interface.

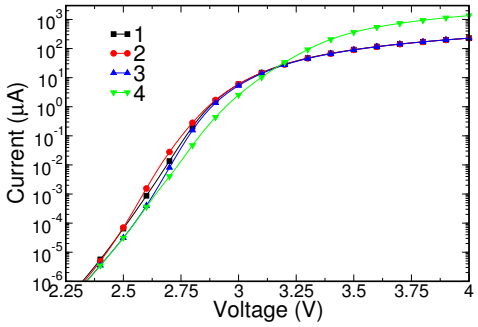

Fig. 2: The simulated IV characteristics for the different nanorods.

Fig. 3 shows the internal quantum efficiency (IQE) calculated classically for the four devices with and without surface recombination. It can be observed that device 2 where the QWs extend to the top polar nanorod surface has clearly the lowest IQE. Moreover, devices 2 and 4 show considerable sensitivity to surface recombination, contrary to the other two. In device 2 this is due to strong strain relaxation at the top nanorod surface, leading to increased carrier densities and thus increased recombination rates. For device 4 the reason is the absence of polarization induced band bending at the bottom interface, which causes an increased hole density and thus increased recombination.

Fig. 4 shows the electron density and current flow lines in the lower part of the nanorod for devices 3 and 4, showing the electron accumulation in device 3 due to the discontinuity in polarization between InGaN/GaN and SiN. This leads to an occupation of the QWs from this interface and a strong axial current component inside the wells. In device 4, electrons enter the MQW stack radially through the potential barrier formed by the leftmost intrinsic GaN barrier, leading to the slightly lower current observed in Fig. 2. In this case, however, the injection into the QWs is more homogeneous

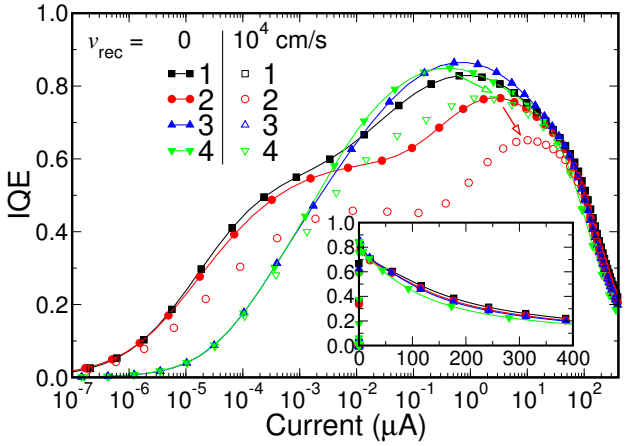

Fig. 3: The simulated IQE for the different nanorods, with and without surface recombination. The inset shows the IQE in linear scale.

along the nanorod, whereas for device 3 one might expect an inhomogeneous emission especially for high aspect ratios. On the other hand, injection from the interfaces increases homogeneity across the QWs, but leads to high local current densities.

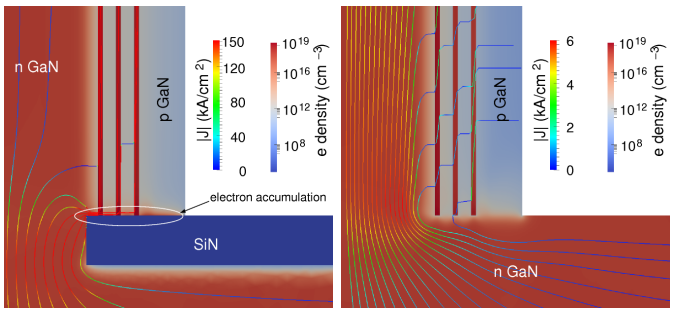

Fig. 4: Electron density and current flow lines in the lower part of the nanorod for (a) device 3 and (b) device 4.

Acknowledgment

The authors thank the EU Project SMASH FP7-228999-2 for support.

References

[1] S. Li and A. Waag, "Gan based nanorods for solid state lighting," *J. Appl. Phys.*, vol. 111, p. 071101, 2012.

[2] M. Deppner, F. Römer, B. Witzigmann, J. Ledig, R. Neumann, A. Waag, W. Bergbauer, and M. Strassburg, "Computational study of carrier injection in iii-nitride core-shell nanowire-leds," in *Semiconductor Conference Dresden (SCD)*, sept. 2011, pp. 1 –4.

[3] C. Mazuir and W. V. Schoenfeld, "Modeling of nitride based core/multishell nanowire light emitting diodes," *Journal of Nanophotonics*, vol. 1, no. 4, p. 0135503, 2007.

[4] B. Connors, M. Povolotskyi, R. Hicks, and B. Klein, "Simulation and design of core-shell gan nanowire leds," in *Proc. SPIE*, vol. 7597, 2010, p. 75970B.

[5] F. Römer, M. Deppner, Z. Andreev, C. Kölper, M. Sabathil, M. Strassburg, J. Ledig, S. Li, A. Waag, and B. Witzigmann, "Luminescence and efficiency optimization of ingan/gan core-shell nanowire leds by numerical modelling," in *Proc. SPIE*, vol. 8255, 2012, p. 82550H.